engineering proceedings

MDPI

Proceeding Paper

Kinematic Design of a Hybrid 2-DoF Ankle Mechanism †

Sayat Akhmejanov [1], Zhanar Bigaliyeva [1], Abu Alim Ayazbay [1,2], Aidos Sultan [2,3], Yerkebulan Nurgizat [2,3], Arman Uzbekbayev [1,2], Kassymbek Ozhikenov [1], Gani Sergazin [3] and Nursultan Zhetenbayev [1,2,3,*]

[1] Department of Robotics and Technical Means of Automation, Satbayev University, Almaty 050013, Kazakhstan; akhmejanov.s@stud.satbayev.university (S.A.); zh.bigaliyeva@satbayev.university (Z.B.); a.ayazbay@aues.kz (A.A.A.); a.uzbekbayev@aues.kz (A.U.); ozhikenov@satbayev.university (K.O.)
[2] Department of Aerospace and Electronic Engineering, Almaty University of Power Engineering and Telecommunications, Almaty 050013, Kazakhstan; a.sultan@aues.kz (A.S.); y.nurgizat@aues.kz (Y.N.)
[3] Department of Science and Innovations, Mukhametzhan Tynyshbayev ALT University, Almaty 050013, Kazakhstan; g.balbayev@alt.edu.kz
* Correspondence: n.zhetenbaev@aues.kz; Tel.: +7-(708)-229-19-00
† Presented at the International Conference on Electronics, Engineering Physics and Earth Science (EEPES2026), Bandirma, Turkey, 24–27 June 2026.

Abstract

This paper presents the kinematic design and experimental validation of a two-degree-of-freedom ankle mechanism based on stepper motor actuation and ball-screw transmission. The proposed system employs a hybrid architecture, combining actively controlled motion in the sagittal plane with passively compliant motion in the frontal plane. Experimental evaluation under no-load laboratory conditions demonstrated a strong linear relationship between motor steps and joint angle within an operating range of approximately $\pm 22°$, with coefficients of determination exceeding 0.97. The results confirm the predictability and repeatability of the kinematic transformation while revealing minor hysteresis effects associated with mechanical transmission. The proposed mechanism is intended as a validation platform for studying motion transformation in multi-DoF (degree-of-freedom) ankle systems, providing a basis for future work on load analysis, torque modeling, and closed-loop control.

Keywords: ankle mechanism; two-degree-of-freedom (2-DoF); kinematic modeling; ball-screw transmission; open-loop control

1. Introduction

Human walking depends on coordinated lower-limb motion, where the ankle joint plays a major role in the stability, propulsion, and regulation of ground reaction forces [1]. For individuals with transtibial amputation, the loss of active ankle push-off increases the metabolic cost of walking and often leads to compensatory gait strategies that overload intact joints [2–4].

Recent advances in powered prosthetic systems have improved the functional capabilities of conventional passive devices. Modern ankle prostheses commonly employ electric actuators and embedded controllers to restore dorsiflexion and plantarflexion motion [5]. However, most commercially available systems remain limited to a single degree of freedom operating only in the sagittal plane [6,7].

In human biomechanics, the ankle also performs inversion and eversion motions in the frontal plane, which are essential for balance control and adaptation to uneven terrain. This

Check for updates

Academic Editors: Teodor Iliev, Ivaylo Stoyanov, Grigor Mihaylov and Selahattin Kosunalp

Published: 7 September 2026

Copyright: © 2026 by the authors. Licensee MDPI, Basel, Switzerland. This article is an open access article distributed under the terms and conditions of the Creative Commons Attribution (CC BY) license.

limitation has motivated the development of multi-degree-of-freedom ankle mechanisms. Several 2-DoF systems have been proposed, including cable-driven and emulator-based designs [8–12]. Although these approaches demonstrated promising performance, many remain mechanically complex, heavy, or limited to laboratory conditions.

Another important challenge is the distribution of mass within the prosthesis. Excessive distal mass increases metabolic cost and negatively affects gait biomechanics [13,14]. Consequently, modern prosthetic designs aim to reduce actuator complexity and overall system weight.

Despite recent progress, the kinematic relationship between actuator input and ankle joint motion is still insufficiently investigated in many existing systems. To address this issue, this study proposes a hybrid two-degree-of-freedom ankle mechanism. In the proposed design, sagittal-plane motion is actively driven using a stepper motor and ball-screw transmission, while frontal-plane mobility is realized passively through the structural configuration of the mechanism. This hybrid approach reduces mechanical complexity while preserving multi-planar motion capability.

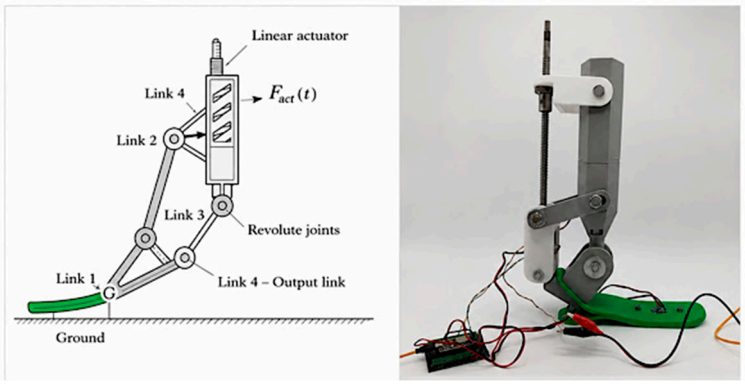
The proposed system is intended as a kinematic validation platform rather than a fully developed clinical prosthesis. The main objective of this work is to experimentally evaluate the relationship between actuator input and ankle joint motion, with particular focus on positioning accuracy, repeatability, and motion linearity.

2. Kinematic Design and Mechanical Architecture of the 2-DoF Ankle Mechanism

The proposed device is a two-degree-of-freedom (2-DoF) ankle mechanism designed to enable motion in two mutually perpendicular planes. From a kinematic point of view, the system can be described as a mechanism with two rotational joints.

The first degree of freedom (R_1) corresponds to motion in the sagittal plane (dorsiflexion–plantarflexion) and is actively driven by a stepper motor through a ball-screw transmission. The second degree of freedom (R_2) represents motion in the frontal plane (inversion–eversion) and is realized passively through the geometry of the mechanism.

The kinematic configuration of the system is illustrated in Figure 1. The diagram shows how the linear motion generated by the actuator is converted into rotational motion at the ankle joint through a multi-link mechanism.



(**a**) (**b**)

Figure 1. Kinematic diagram and experimental prototype of the two-degree-of-freedom ankle mechanism: (**a**) kinematic diagram; (**b**) experimental prototype.

The mobility of the mechanism can be estimated using the Grübler–Kutzbach criterion:

$$M = 3(n - 1)\text{-}2j_1 - j_2 \quad (1)$$

where n is the number of links and j_1 is the number of single-degree-of-freedom joints.

Since all joints in the proposed design are revolute, the overall mobility of the system is $M = 2$. This corresponds to two independent rotational motions in the sagittal and frontal planes.

Motion in the sagittal plane is generated through the ball-screw transmission. The rotation of the stepper motor produces a linear displacement along the screw:

$$\Delta x = p \cdot N \tag{2}$$

where p is the screw pitch and N is the number of motor steps. This linear displacement is then converted into angular rotation through the linkage mechanism, which can be approximated (for small angles) as:

$$\theta \approx \Delta x / r \tag{3}$$

where r is the effective lever arm. As a result, the overall kinematic transformation follows a clear sequence: motor steps, linear displacement, linkage motion, joint rotation. This relationship is deterministic and forms the basis for the experimental validation presented later.

The experimental prototype shown in Figure 1b integrates the stepper motor, ball-screw transmission, and linkage system to produce controlled angular motion of the foot segment. The actuator is positioned away from the joint axis, which helps reduce distal mass and improves the overall dynamic characteristics of the system.

The motion in the frontal plane (R_2) is not directly actuated. Instead, it arises from the geometric configuration of the mechanism and its interaction with external forces. In practice, this motion is influenced by ground reaction forces and the contact between the foot segment and the supporting surface.

The spatial arrangement of the rotational axes is designed so that they intersect near the geometric center of the ankle joint. This helps reduce unwanted parasitic motion and brings the mechanism closer to the natural biomechanics of the human ankle.

Overall, the proposed design can be described as a hybrid kinematic system with two degrees of freedom, where one axis is actively controlled and the other is realized passively. This approach reduces structural complexity while still allowing multi-planar motion, and it provides a clear framework for analyzing and experimentally validating the kinematic transformation.

3. Actuation and Control Architecture of the Ankle Mechanism

The actuation and control system of the proposed ankle mechanism is based on stepper motor-driven position control and is implemented using a custom-designed embedded platform. The complete electrical schematic of the system is shown in Figure 2, while the physical realization of the control board is presented in Figure 3.

At the core of the control system is an ESP32-S3 microcontroller (Espressif Systems, Shanghai, China), which handles motor control, sensor data processing, and communication with external devices. The electrical design separates the power and logic domains (5 V and 3.3 V), which helps ensure stable operation and reduces the influence of electrical noise. Power is supplied via a USB-C interface, while a CH340 USB-to-UART converter (Nanjing Qinheng Microelectronics, Nanjing, China) is used for programming and data exchange.

The stepper motor is controlled using STEP and DIR signals. The STEP signal defines the discrete movement increments of the motor, while the DIR signal determines the direction of rotation. These signals are generated by the microcontroller and sent to an external driver, which regulates the current and controls the excitation of the motor windings. In this configuration, the system operates in an open-loop mode, where the position is determined by counting motor steps.

https://doi.org/10.3390/engproc2026154052

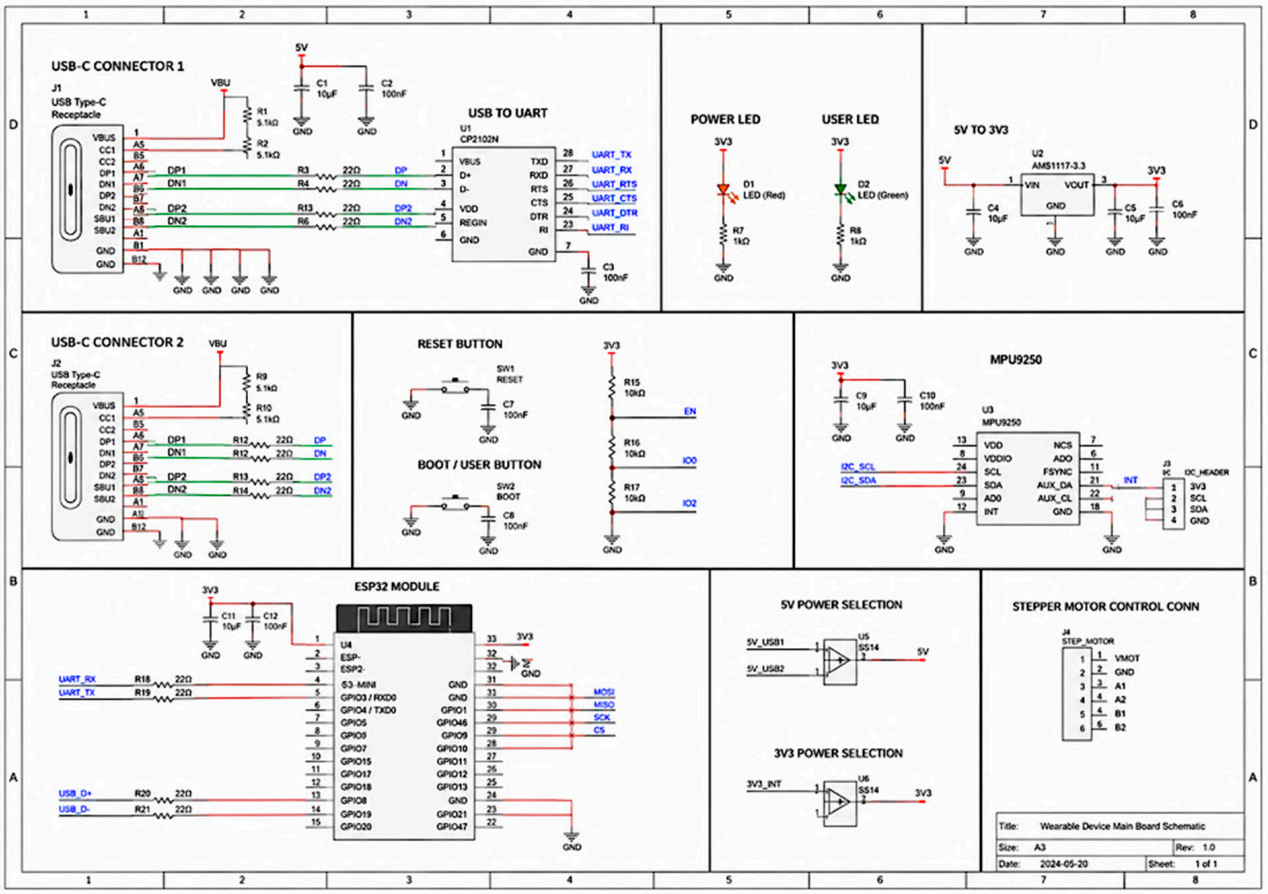


Figure 2. Electrical schematic of the ankle mechanism control system including the ESP32, power supply, inertial measurement unit IMU, and interface components. Colors distinguish the electrical connections, while the letters and numbers indicate component designations, pin numbers, signal names, and voltage levels.

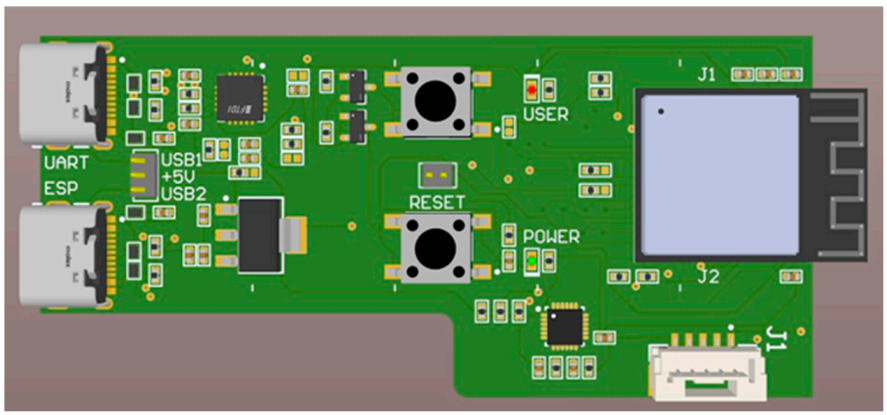


Figure 3. Custom-designed control board (PCB) used for stepper motor actuation. The labels identify the main connectors, controls, and electronic components, while the colors are used only for visual representation and do not encode additional information.

Although open-loop stepper motor systems may be susceptible to step-skipping under excessive load conditions, the proposed mechanism was operated at low angular velocities and moderate torque levels to minimize this risk. In addition, the selected motor provided sufficient torque margin relative to the required ankle actuation load. During the experimental trials, no observable synchronization loss or positioning instability was detected. The implemented homing procedure using a mechanical limit switch also improved re-

peatability by re-establishing the reference position before each experiment. Nevertheless, the integration of encoder-based closed-loop feedback control will be considered in future work to further improve positioning reliability and robustness.

The rotational motion of the motor is converted into linear displacement through a ball-screw mechanism. This linear motion is then transformed into angular rotation of the ankle joint via the multi-link mechanism described in Section 2. As a result, the actuation system establishes a deterministic geometric transformation chain from motor steps to joint angle.

To measure angular displacement, an MPU9250 inertial measurement unit (IMU; TDK InvenSense, San Jose, CA, USA) is used. The sensor communicates with the microcontroller via the I^2C interface and provides real-time measurements of angular velocity and linear acceleration. These data are used to estimate the ankle joint angle. It is important to note that the IMU is not used for feedback control; instead, it is employed solely for experimental validation and measurement purposes. This allows the kinematic behavior of the mechanism to be evaluated independently of any control-loop effects.

A homing procedure based on a mechanical limit switch is used to define the initial reference position of the system. At startup, the mechanism is moved to a known zero position, and all subsequent motion is defined relative to this reference. This approach improves positioning accuracy and ensures repeatability across multiple experimental trials.

The control board shown in Figure 2 integrates all key components into a compact and modular design, including the microcontroller, power management circuitry, user interface elements, and motor driver connections. This modular architecture leaves room for future extensions, such as closed-loop control, additional sensing, and more advanced control strategies.

Overall, the proposed actuation and control system is fully defined from electrical, logical, and functional perspectives. It provides a reliable platform for studying the kinematic transformation, positioning accuracy, and repeatability of the ankle mechanism under controlled laboratory conditions.

4. Control and Measurement Architecture

The control and measurement architecture of the proposed ankle mechanism is designed to ensure precise and repeatable motion generation, while also enabling quantitative evaluation of its kinematic performance. The overall system configuration is illustrated in Figure 4.

Within this architecture, an ESP32-based embedded controller serves as the central control unit, generating STEP and DIR signals for the stepper motor driver. These signals are produced according to predefined motion profiles and enable discrete position control of the actuator. The system operates in an open-loop mode, meaning that the joint position is determined by the number of commanded motor steps.

To establish a consistent reference, a homing procedure is performed at startup. This process relies on a mechanical limit switch, which defines a repeatable zero position for the mechanism. Once the homing sequence is completed, the internal step counter of the controller tracks all subsequent motion relative to this reference. This approach ensures a high level of repeatability during experimental trials.

Angular motion is measured using an MPU9250 inertial measurement unit (IMU) mounted on the foot segment. The sensor communicates with the controller via the I^2C interface and provides real-time orientation data. These measurements are used exclusively for experimental analysis and are not fed back into the motor control loop. This separation allows for the kinematic behavior of the mechanism to be evaluated independently of control-related effects.

https://doi.org/10.3390/engproc2026154052

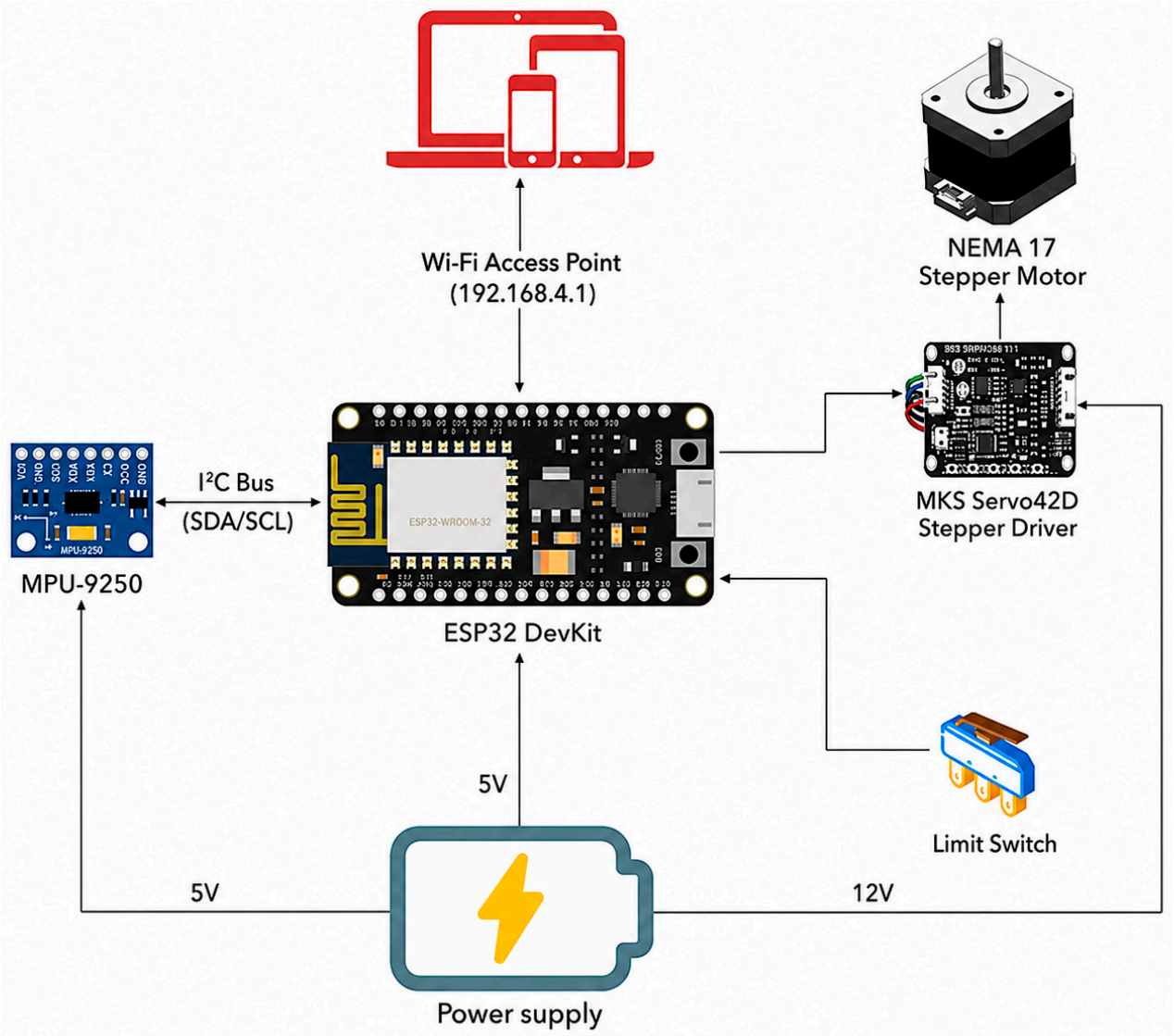


Figure 4. Control and measurement architecture of the ankle mechanism, including stepper motor control, homing procedure, IMU-based angle measurement, and wireless communication interface.

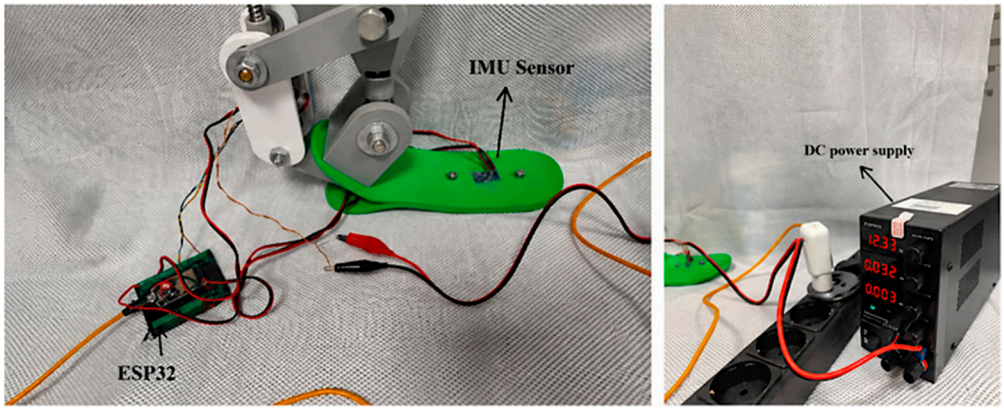
In addition, the system includes a built-in Wi-Fi module that enables wireless communication. This allows external devices to send motion commands and monitor system performance during testing. The communication layer functions purely as an interface and does not alter the open-loop nature of the position control.

Overall, the proposed architecture combines reference-based positioning (through homing and step counting) with independent angular measurement. This clear separation between control and measurement provides a transparent experimental framework for analyzing motion linearity, repeatability, and potential hysteresis effects without introducing additional complexity from closed-loop control.

5. Experimental Results and Validation of Kinematic Performance

The experimental evaluation of the proposed two-degree-of-freedom ankle mechanism was carried out to assess the accuracy of the kinematic transformation, positioning repeatability, and motion linearity. All experiments were conducted under controlled laboratory conditions without external load (no-load condition), allowing the geometric relationship between actuation and joint motion to be examined independently.

The experimental setup is shown in Figure 5. The mechanism was rigidly fixed to a stationary base in order to minimize external disturbances and unwanted motion. The system was driven by a stepper motor controlled via an ESP32-based embedded unit. A regulated DC power supply was used to ensure stable operation of both the motor driver and the control electronics. Angular displacement was measured using an MPU9250 inertial measurement unit (IMU) mounted directly on the foot segment, enabling direct measurement of the ankle joint orientation.

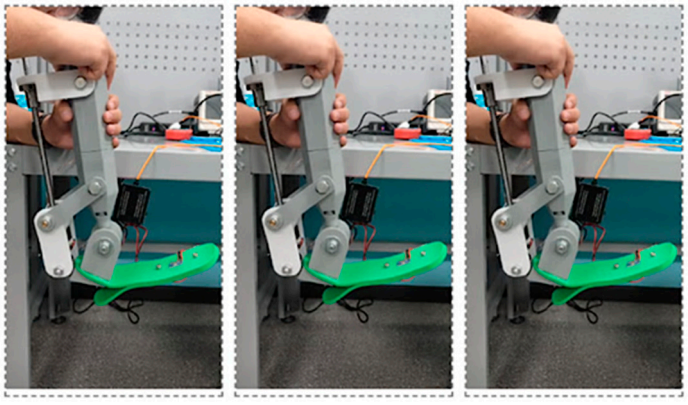


(**a**) (**b**)

Figure 5. Experimental setup of the 2-DoF ankle mechanism: (**a**) ankle mechanism with IMU-mounted foot segment and embedded controller; (**b**) external DC power supply used during experiments.

The experimental protocol focused on controlled motion in the sagittal plane within an operating range of approximately ±22°. Motion was executed in both directions: downward (plantarflexion-dominant) and upward (dorsiflexion-dominant). This approach allowed for the symmetry of the system and potential hysteresis effects to be evaluated. Each test was performed after a homing procedure, and all measurements were referenced to the same initial zero position.

Representative positions of the mechanism during operation are shown in Figure 6. The images correspond to different commanded step inputs within the working range. The sequence demonstrates smooth and continuous motion, with no visible mechanical locking or abrupt transitions. No noticeable structural deformation or joint misalignment was observed within the tested range. Repeatability was assessed through multiple forward–reverse cycles, during which the mechanism consistently returned to the same zero reference position, indicating stable step-based positioning.



(**a**) (**b**) (**c**)

Figure 6. Experimental sequence of ankle mechanism motion: (**a**) neutral position; (**b**) dorsiflexion motion; (**c**) plantarflexion motion.

https://doi.org/10.3390/engproc2026154052

To quantify the system behavior, a regression analysis was performed between the number of motor steps and the corresponding joint angle measured by the IMU. The results for the downward motion are presented in Figure 7.

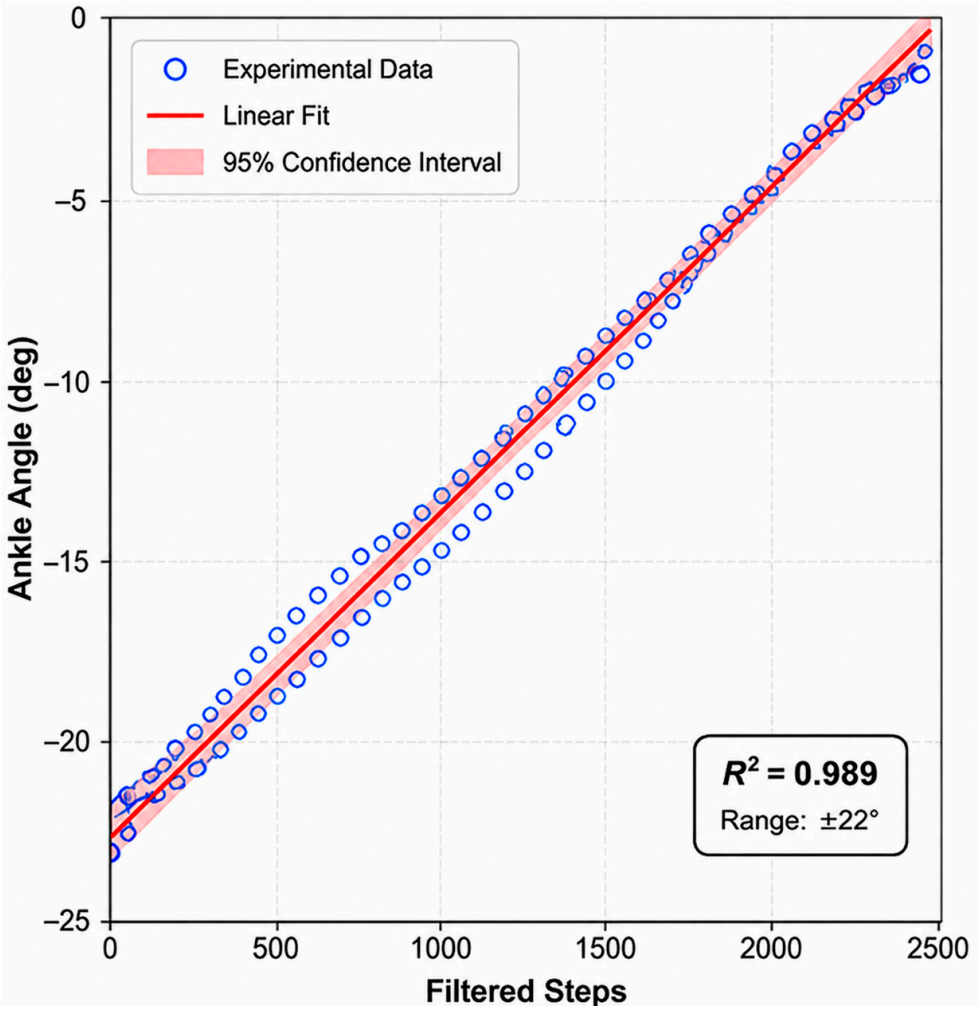


Figure 7. Correlation between motor steps and ankle joint angle during downward motion (plantarflexion-dominant) with linear regression (R^2 = 0.989).

Prior to regression analysis, the experimentally measured IMU signals were filtered in order to reduce high-frequency noise and sensor fluctuations. As a result, the number of filtered data samples differed from the number of commanded motor steps. The motor input itself remained deterministic and was generated directly by the stepper controller, while the filtering procedure was applied only to the measured angular response. This preprocessing improved the stability of the regression analysis and reduced the influence of measurement noise on the estimated kinematic relationship.

The data showed a strong linear relationship with a coefficient of determination of R^2 = 0.989, indicating that approximately 98.9% of the angular variation can be explained by the motor input. The remaining deviation was attributed to measurement noise and minor nonlinearities in the mechanical transmission. The results for the upward motion are shown in Figure 8.

In this case, the linear relationship remained strong, although the coefficient of determination was slightly lower (R^2 = 0.972). This difference suggests the presence of minor hysteresis effects, which are likely caused by backlash and friction within the ball-screw and linkage mechanism. Such behavior is typical for mechanical systems of this type.

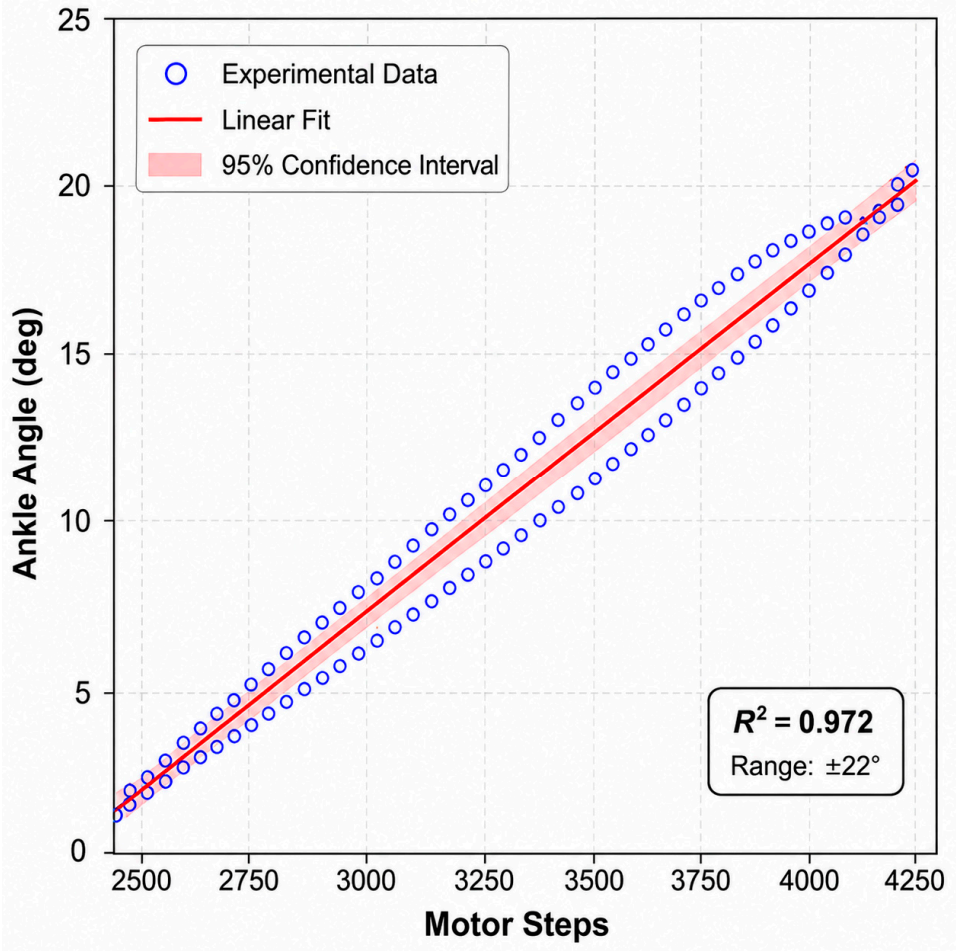


Figure 8. Correlation between motor steps and ankle joint angle during upward motion (dorsiflexion-dominant) with linear regression (R^2 = 0.972).

Overall, the high values of $R^2 > 0.97$ in both directions confirm the linearity and predictability of the motion transformation, as well as the consistency of the positioning within the tested range. The observed asymmetry between forward and reverse motion remained relatively small and within acceptable limits for a prototype-level system.

To evaluate repeatability and positioning consistency, multiple forward–reverse experimental cycles were performed under identical operating conditions. The validation criteria included repeatability of the zero reference position, smoothness of motion, absence of observable step loss, and linear correlation between motor input and measured ankle angle. Linear regression analysis was used as the primary statistical evaluation method, where the coefficient of determination (R^2) quantified the strength of the kinematic relationship between commanded motor steps and joint motion.

It should be emphasized that these results reflect kinematic performance under no-load conditions and do not represent the behavior of the mechanism under realistic gait loading. Therefore, the current study did not address force generation, torque output, or dynamic interaction with the ground. Instead, the results should be interpreted as a validation of the underlying kinematic transformation. As such, they provide a useful experimental basis for future work involving load analysis, torque modeling, and the development of closed-loop control strategies.

6. Discussion

The experimental study was aimed at evaluating the accuracy of the kinematic transformation between actuator input and joint motion in the proposed two-degree-of-freedom

ankle mechanism. The results showed a strong linear relationship between the number of motor steps and the resulting joint angle, with coefficients of determination of $R^2 = 0.989$ for downward motion and $R^2 = 0.972$ for upward motion. These values indicate that the angular displacement is largely governed by the commanded step sequence, confirming good positioning accuracy of the system.

The slight difference in R^2 values between forward and reverse motion suggests the presence of hysteresis effects within the mechanism. This behavior is typical for systems involving ball-screw transmissions and linkage mechanisms, and can be attributed to backlash, friction, and material compliance. However, the observed deviations were relatively small compared to the overall working range (approximately $\pm 22^\circ$) and did not significantly affect motion stability or continuity.

The achieved angular range of approximately $\pm 22^\circ$ represents a partial reproduction of the physiological ankle motion range. In healthy human biomechanics, the ankle joint typically allows for approximately 20° of dorsiflexion and up to 45° of plantarflexion. Therefore, the proposed mechanism does not yet cover the complete natural ankle range of motion. Nevertheless, the obtained motion range is sufficient for validating the kinematic transformation principles and for performing controlled laboratory-scale rehabilitation and assistive motion experiments. Future optimization of the linkage geometry and actuator stroke may allow for expansion of the achievable angular range toward more physiologically representative motion.

From a biomechanical perspective, the human ankle does not operate solely in the sagittal plane but also plays an active role in the frontal plane, contributing to balance control and the regulation of ground reaction forces. In the proposed mechanism, motion in the sagittal plane is actively driven, while motion in the frontal plane is realized passively through the structural configuration. This hybrid approach reduces system complexity compared to fully actuated designs and helps limit distal mass, which is an important factor for improving biomechanical efficiency. In addition, the spatial arrangement of the rotational axes, positioned near the geometric center of the joint, helps reduce parasitic motion and better approximate natural ankle behavior.

At the same time, the results should not be interpreted as evidence of full biomechanical equivalence. The experiments were conducted under no-load and stationary laboratory conditions, meaning that the findings primarily reflect the accuracy of the kinematic transformation. In real gait, the ankle is subject to complex dynamic loading, where torque generation and interaction with ground reaction forces play a critical role. These aspects were not addressed in the present study and remain topics for future investigation.

It should also be noted that although the system was designed with two degrees of freedom, the experimental validation focused mainly on motion in the sagittal plane. While frontal-plane motion is supported by the kinematic structure, its detailed experimental characterization and control have not yet been explored. For this reason, the proposed system should be viewed not as a fully functional 2-DoF prosthetic device, but rather as an initial platform for validating the underlying kinematic principles.

The main contribution of this work lies in the experimental verification of a deterministic kinematic transformation chain linking motor steps, linear displacement, linkage motion, and joint rotation. The observed linear relationship between input and output demonstrates that the mechanism can be controlled in a predictable and repeatable manner. This provides a solid basis for future studies involving force analysis, torque estimation, and the development of closed-loop control strategies.

In this sense, the presented system is better understood as an experimental platform for studying motion transformation in multi-DoF ankle mechanisms rather than as a finalized clinical solution. The results offer quantitative evidence of kinematic performance and

can support further development toward systems capable of operating under realistic biomechanical conditions.

7. Conclusions

This paper presented the kinematic design and experimental validation of a two-degree-of-freedom ankle mechanism based on a stepper motor and ball-screw transmission. The proposed design follows a hybrid architecture, with actively controlled motion in the sagittal plane and passively compliant motion in the frontal plane. This approach helps reduce structural complexity while maintaining a clear and well-defined kinematic transformation.

Experimental results obtained under laboratory conditions showed a strong linear relationship between motor steps and ankle joint angle. Within the tested operating range of approximately $\pm 22^{\circ}$, the coefficient of determination exceeded $R^2 > 0.97$ in both motion directions, indicating good positioning accuracy and a predictable transformation between input and output. A small difference between forward and reverse motion suggests the presence of limited hysteresis, which can be attributed to friction and backlash within the transmission system.

It should be noted that these results do not represent the dynamic or load-bearing performance of a fully functional prosthetic device. The study was focused on evaluating kinematic transformation accuracy and positioning repeatability under no-load conditions, without considering external forces or realistic gait scenarios. For this reason, the proposed system should be viewed as an experimental platform for studying kinematic behavior in multi-degree-of-freedom mechanisms, rather than as a complete clinical solution.

The main contribution of this work lies in the quantitative verification of the kinematic transformation chain from motor steps to joint rotation (motor steps, linear displacement, linkage motion, joint angle). The results provide a reliable experimental basis for assessing motion linearity, positioning accuracy, and repeatability.

Future work will focus on evaluating the force and dynamic characteristics of the mechanism, including its behavior under loading conditions, as well as the integration of feedback-based control strategies. In addition, further investigation of frontal-plane motion and its biomechanical relevance will be an important direction for subsequent studies.

Author Contributions: Conceptualization, N.Z., S.A. and A.S.; methodology, N.Z., A.S., Z.B., A.A.A. and A.U.; mathematical modeling, S.A., K.O. and Z.B.; software, N.Z., Z.B., Y.N. and A.U.; validation, N.Z., S.A., A.S., Y.N. and A.U.; formal analysis, N.Z. and K.O.; investigation, N.Z., Z.B., A.A.A., Y.N. and A.U.; resources, G.S. and A.S.; data curation, N.Z. and Y.N.; writing—original draft preparation, N.Z.; writing—review and editing, N.Z., G.S., S.A. and A.S.; visualization, Z.B. and Y.N.; supervision, G.S. and N.Z.; project administration, N.Z.; funding acquisition, G.S. All authors have read and agreed to the published version of the manuscript.

Funding: This research was funded by the Science Committee of the Ministry of Science and Higher Education of the Republic of Kazakhstan within the framework of the program BR24992820.

Institutional Review Board Statement: Not applicable.

Informed Consent Statement: Not applicable.

Data Availability Statement: The data presented in this study are available on request from the corresponding author.

Conflicts of Interest: The authors declare no conflicts of interest.

References

1. Ficanha, E.M.; Ribeiro, G.A.; Dallali, H.; Rastgaar, M. Design and preliminary evaluation of a two DOF cable-driven ankle–foot prosthesis with active dorsiflexion–plantarflexion and inversion–eversion. *Front. Bioeng. Biotechnol.* **2016**, *4*, 36. [CrossRef]

2. Kaufman, K.R.; Levine, J.; Brey, R.; McCrady, S.; Padgett, D.; Joyner, M. Energy Expenditure and Activity of Transfemoral Amputees Using Mechanical and Microprocessor-Controlled Prosthetic Knees. *Arch. Phys. Med. Rehabil.* **2008**, *89*, 1380–1385. [CrossRef]
3. Xu, H.; Feng, Z.; Dou, Y.; Wang, G. Effects of a 6-Week Hip and Ankle Mobility-Based Rehabilitation Program on Clinical, Neuromuscular, and Functional Outcomes in Male Collegiate Athletes with Patellofemoral Pain: A Randomized Controlled Trial. *Life* **2026**, *16*, 1013. [CrossRef]
4. Ventura, J.D.; Segal, A.D.; Klute, G.K.; Neptune, R.R. Compensatory mechanisms of transtibial amputees during circular turning. *Gait Posture* **2011**, *34*, 307–312. [CrossRef]
5. Sultan, A.; Zhetenbayev, N.; Nurgizat, Y.; Ayazbay, A.; Ozhikenov, K.; Sergazin, G. Analysis of the lower limb prosthesis market and a research of advanced prosthetic methods. In *New Trends in Medical and Service Robotics*; Laribi, M.A., Carbone, G., Pisla, D., Zeghloul, S., Eds.; Springer: Cham, Switzerland, 2025; Volume 186. [CrossRef]
6. Glaister, B.C.; Bernatz, G.C.; Klute, G.K.; Orendurff, M.S. Video task analysis of turning during activities of daily living. *Gait Posture* **2007**, *25*, 289–294. [CrossRef]
7. Ficanha, E.M.; Rastgaar, M.; Kaufman, K.R. A two-axis cable-driven ankle-foot mechanism. *Rob. Biomim.* **2014**, *1*, 17. [CrossRef]
8. Bellman, R.D.; Holgate, M.A.; Sugar, T.G. SPARKy 3: Design of an active robotic ankle prosthesis with two actuated degrees of freedom using regenerative kinetics. In Proceedings of the IEEE/RAS-EMBS International Conference on Biomedical Robotics and Biomechatronics, Scottsdale, AZ, USA, 19–22 October 2008; pp. 511–516.
9. Ficanha, E.M.; Rastgaar, M.; Kaufman, K.R. Ankle mechanics during sidestep cutting implicates the need for 2-DOF powered ankle–foot prostheses. *J. Rehabil. Res. Dev.* **2015**, *52*, 97–112. [CrossRef]
10. Ficanha, E.M.; Rastgaar, M.; Kaufman, K.R. Control of a 2-DOF powered ankle-foot mechanism. In Proceedings of the IEEE International Conference on Robotics and Automation (ICRA), Seattle, WA, USA, 26–30 May 2015.
11. Kim, M.; Chen, T.; Chen, T.; Collins, S.H. An ankle–foot prosthesis emulator with control of plantarflexion and inversion–eversion torque. *IEEE Trans. Robot.* **2018**, *34*, 1183–1194. [CrossRef]
12. Jang, W.-S.; Kim, D.Y.; Choi, Y.S.; Kim, Y.J. Self-contained 2-DOF ankle–foot prosthesis with low-inertia extremity for agile walking on uneven terrain. *IEEE Robot. Autom. Lett.* **2021**, *6*, 8134–8141. [CrossRef]
13. Browning, R.; Modica, J.; Kram, R.; Goswami, A. The effects of adding mass to the legs on the energetics and biomechanics of walking. *Med. Sci. Sports Exerc.* **2007**, *39*, 515. [CrossRef] [PubMed]
14. Dygut, J.M.; Piwowar, M.W. Pressure Force in the Upper Ankle Joint. *Appl. Sci.* **2025**, *15*, 11230. [CrossRef]

Disclaimer/Publisher's Note: The statements, opinions and data contained in all publications are solely those of the individual author(s) and contributor(s) and not of MDPI and/or the editor(s). MDPI and/or the editor(s) disclaim responsibility for any injury to people or property resulting from any ideas, methods, instructions or products referred to in the content.